LAWRENCE
LIVERMORE
NATIONAL
LABORATORY

UCRL-PROC-221295

Development and Characterization of a High Magnetic Field Solenoid for Laser Plasma Experiments

B. B. Pollock, D. H. Froula, P. F. Davis, J. S. Ross, L. Divol, S. Fulkerson, J. Satariano, D. Price, J. Bower, J. Edwards, R. Town, S. H. Glenzer, A. A. Offenberger, G. R. Tynan, A. N. James

May 10, 2006

High Temperature Plasma Diagnostics
Willliamsburg, VA, United States
May 7, 2006 through May 11, 2006

Disclaimer

Development and Characterization of a High Magnetic Field Solenoid for Laser Plasma Experiments

B. B. Pollock,* D. H. Froula, P. F. Davis,† J. S. Ross, L. Divol, S. Fulkerson, J. Satariano, D. Price, J. Bower, J. Edwards, R. Town, and S. H. Glenzer
Lawrence Livermore National Laboratory, University of California, P.O. Box 808, Livermore, California 94551

A. A. Offenberger
Department of Electrical Engineering, University of Alberta, Edmonton, Alberta, Canada T6G 2V4

G. R. Tynan and A. N. James
Department of Mechanical and Aerospace Engineering, University of California San Diego
(Date textdate; Received textdate; Revised textdate; Accepted textdate; Published textdate)

An electromagnetic solenoid was developed to study the quenching of nonlocal heat transport in laser-produced gas-jet plasmas by high external magnetic fields. The solenoid, which is driven by a pulsed power system supplying 30 kJ, achieves fields exceeding 10 T. Temporally resolved measurements of the electron temperature profile transverse to a high power laser beam were obtained using Thomson Scattering. A method for optimizing the solenoid design based on the available stored energy is presented.

PACS numbers:

I. INTRODUCTION

Magnetic fields play a significant role in the physical behavior of plasmas relevant to Inertial Confinement Fusion (ICF), such as those produced at the National Ignition Facility (NIF)[1]. Specifically, magnetic fields effect electron heat transport within the plasma[2]. The properties of heat transport are of particular importance in understanding the spatial temperature dependence in ICF plasmas[3].

The presence of a strong background magnetic field during laser-plasma formation causes ionized electrons to perform gyro-orbits in the plane perpendicular to the applied field due to the Lorentz force. The Larmor radius ($r_L = mv/eB$) of this cyclotron motion is much shorter than the temperature scale length of the plasma, preventing hot electrons from colliding with cold plasma outside of the pressure-driven heat front. This confinement of electrons means that the Braginskii heat transport equations are applicable, and that the expansion of the heat front is slowed due to a lack of pre-heating. Our experiment utilizes a 12 T background field, which successfully inhibits thermal transport away from the laser heated region of the plasma. The peak electron temperature increases from 250 eV without an external field to 850 eV when the 12 T field is applied, and the heat wave propagation is considerably delayed[4].

In order to significantly inhibit thermal transport in our laser-produced plasmas, magnetic fields greater than 10 T are necessary[4]. While a conventional Bitter electromagnet[5] is capable of producing such fields, the operating environment of our experiment demanded certain modifications be made. We have developed a solenoid comprised of two modified Bitter electromagnets constructed in series, allowing access to the high magnetic field for diagnostics, laser beams, and a gas jet (Figure 1)[6].

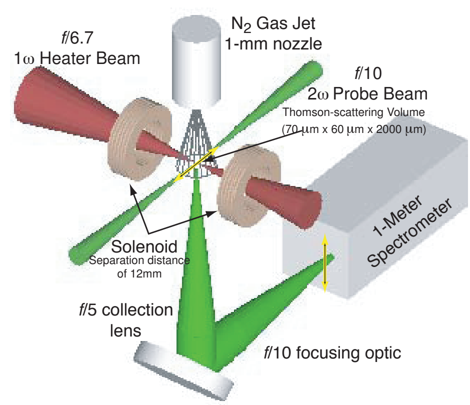

FIG. 1: The schematic for the laser setup is shown. A 12 mm gap between the coils allows access to the high magnetic fields. The system has been optimized to provide high fields directly between the coils.

II. LASER PLASMA EXPERIMENT

The laser plasma experiment performed at the Janus Laser Facility, Lawrence Livermore National Laboratory, employed a gas jet to deliver N_2 gas that is heated by a high power (1 ns) laser beam with 100 J of 1 ω (1053 nm)

*School of Engineering and Computer Science, University of the Pacific, Stockton, CA 95211
†Department of Physics, University of British Columbia, Vancouver, Canada, V2T 6W9

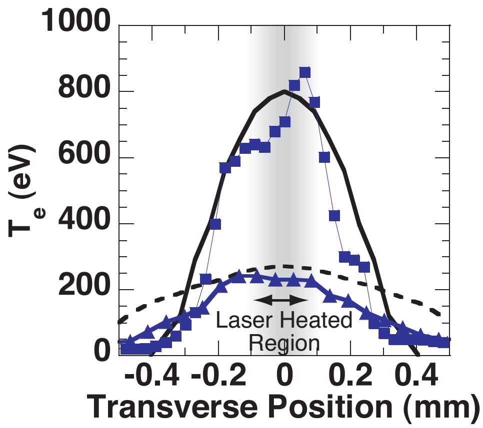

FIG. 2: The electron temperature profiles for no magnetic field (triangles) and an externally applied field of 12 T (squares) show an increase in peak electron temperature and a corresponding reduction in the propagation of the heat wave perpendicular to the magnetic field. LASNEX simulations using a flux-limited diffusion model (f=1) without magnetic fields (dashed line) underestimate the extent of the heat wave, consequently simulating a higher peak electron temperature. Simulations using the magnetic field package (solid line) accurately reproduce the experimental results.

light in the presence of an external magnetic field. Imaging Thomson Scattering with 500 mJ of 2 ω (527 nm) light is used to spatially resolve the electron temperature profile perpendicular to the heater beam.

Figure 2 compares the electron temperature profiles with and without a magnetic field 500 ps after the rise of the heater beam. The profile for the spectrum observed with no applied field shows that the heat front extends out well past 500 microns from the center of the heater beam. This is in stark contrast to the high field (B=12 T) case, where the heat front has propagated less than 350 microns. This is direct evidence of reduction in electron heat flux by an external magnetic field.

The results presented in Figure 3 are compared to simulations using the hydrodynamic code LASNEX[7] where the classical heat transport equations presented by Braginskii[8] are solved. The simulations agree well with the data when a background field is present. For our conditions without magnetic fields, it has been previously shown that classical diffusion is not able to reproduce the heat wave propagation even when a flux limiter is used, and that nonlocal transport effects play an important role in the calculation of plasma conditions[9]. Figure 3 reproduces these results showing that the Braginskii diffusion model that includes self-generated magnetic fields does not correctly calculate the electron temperature profile when no external magnetic field is present. The comparison shows that self-generated magnetic fields do not account for the nonlocal nature of the heat flux.

III. MAGNETIC FIELD GENERATION

A solenoid is constructed from two coils in series with a gap between them to allow access for a laser plasma interaction experiment. The field between the coils has been designed to be greater than 10 T using a stored energy of 30 kJ. We have developed a model that shows that for systems with less than 50 kJ of stored energy there is an optimal solenoid design, limited by the material strength of copper, providing a 20 T field between the coils. To achieve fields greater than this threshold, the optimal design is chosen by the total stored energy.

The solenoid is driven by a pulse power system, where it is placed in series with a capacitor bank capable of delivering 28.8 kJ when charged to 20 kV. The resulting LRC circuit is underdamped, and the current output is well characterized[6]. To determine the magnetic field along the axis a 10 turn, 1.5 mm diameter pickup probe was constructed and calibrated. Figure 3a shows the measured magnetic field strength between the coils for the maximum capacitor charge of 20 kV as compared with analytical calculations. Figure 3b compares the peak magnetic field recorded along the solenoid axis for a constant capacitor charge of 1 kV with the calculated magnetic field profile.

The current through an LRC system is a function of the charge voltage, capacitance, resistance, and inductance. The inductance can be calculated as a function of the number of turns and the inner solenoid radius[6], which allows us to optimize the current through the solenoid by varying these parameters. Using the peak current generated by a critically damped LRC circuit normalized by the total stored energy $\left(J_{peak} = \frac{I_{peak}}{\sqrt{E}} = \sqrt{\frac{2}{e^2 L(N,r)}}\right)$, the magnetic field between the coils can be expressed[6],

$$H(N,r) = J_{peak}G(0) = \sqrt{\frac{2}{e^2 L(N,r)}} \times \frac{\mu_0 N}{2l}\left(\frac{l+\frac{d}{2}}{\sqrt{r^2+(l+\frac{d}{2})^2}} - \frac{\frac{d}{2}}{\sqrt{r^2+(\frac{d}{2})^2}}\right) \tag{1}$$

where $H = \frac{B}{\sqrt{E}}$ is the normalized magnetic field strength and $E = \frac{1}{2}CV_0^2$ is the stored energy in the system.

Figure 4a is a contour plot of Equation 1, given that the coils are 12 mm apart, each turn is 627 μm thick, and that the system adds 4 μH of stray inductance. The black curves represent solenoid geometries that produce the same current, while the orange line passes through the point on each curve corresponding to its highest magnetic field. The optimal system design corresponds to the maximum of Equation 1. Figure 4b plots the peak field between the coils, the peak field inside the solenoid, and the ratio of these two. If the desired field strength between the coils raises the peak field inside the solenoid above the material limit of the solenoid (approximately 30 T for copper) the appropriate ratio must be chosen,

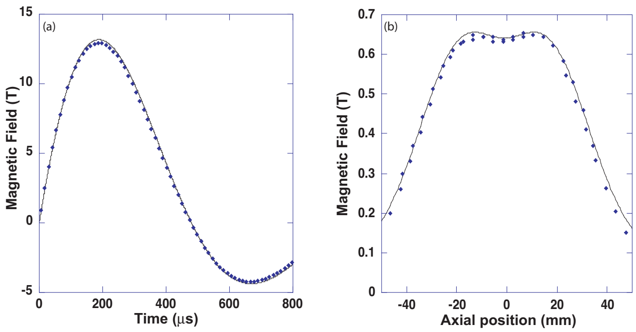

FIG. 3: (a) The magnetic field is measured at the center of the solenoid using a pick-up probe. (b) The magnetic field along the axis of the solenoid shows a maximum field inside the coils and a slight dip in the profile between the coils. Analytical models are included in both plots.

which determines the system geometry and sets the maximum field that can be achieved.

We would like to thank the Janus Laser Crew for their outstanding support during our campaign. This work was performed under the auspices of the U.S. Department of Energy by the Lawrence Livermore National Laboratory under Contract No. W-7405-ENG-48.

[1] J. D. Lindl, P. A. Amendt, R. L. Berger, S. G. Glendinning, S. H. Glenzer, S. W. Haan, R. L. Kauffman, O. L. Landen, and L. J. Suter, Phys. Plasmas **11**, 339 (2004).

[2] P. D. Nicolai, J. L. A. Feugeas, and G. P. Schurtz, Phys. Plasmas **13**, 2701 (2006).

[3] S. H. Glenzer, W. E. Alley, K. G. Estabrook, J. S. D. Groot, M. G. Haines, J. H. Hammer, J. P. Jadaud, B. J. MacGowan, J. D. Moody, W. Rozmus, et al., Phys. Plasmas **6** (1999).

[4] D. H. Froula, P. F. Davis, B. B. Pollock, L. Divol, J. S. Ross, J. Edwards, R. P. J. Town, D. Price, S. H. Glenzer, A. A. Offenberger, et al., Submitted to PRL (2006).

[5] F. Bitter, Rev. Sci. Instrum. **10**, 373 (1939).

[6] B. B. Pollock, P. F. Davis, D. H. Froula, J. S. Ross, R. Kingham, S. Fulkerson, J. Bower, J. Satariano, S. H. Glenzer, and D. Price, To Be published in RSI (2006).

[7] G. B. Zimmerman and W. L. Kruer, Comments Plasma Physics and Controlled Fusion **2**, 51 (1975).

[8] S. I. Braginskii, Zh. Eksp. Teor. Fiz. **33**, 459 (1957).

[9] G. Gregori, S. H. Glenzer, J. Knight, C. Niemann, D. Price, D. H. Froula, M. J. Edwards, R. P. J. Town, W. Rozmus, A. Brantov, et al., Phys. Rev. Lett. **92** (2004).

This work was performed under the auspices of the U. S. Department of Energy by University of California, Lawrence Livermore National Laboratory under contract W-7405-Eng-48.

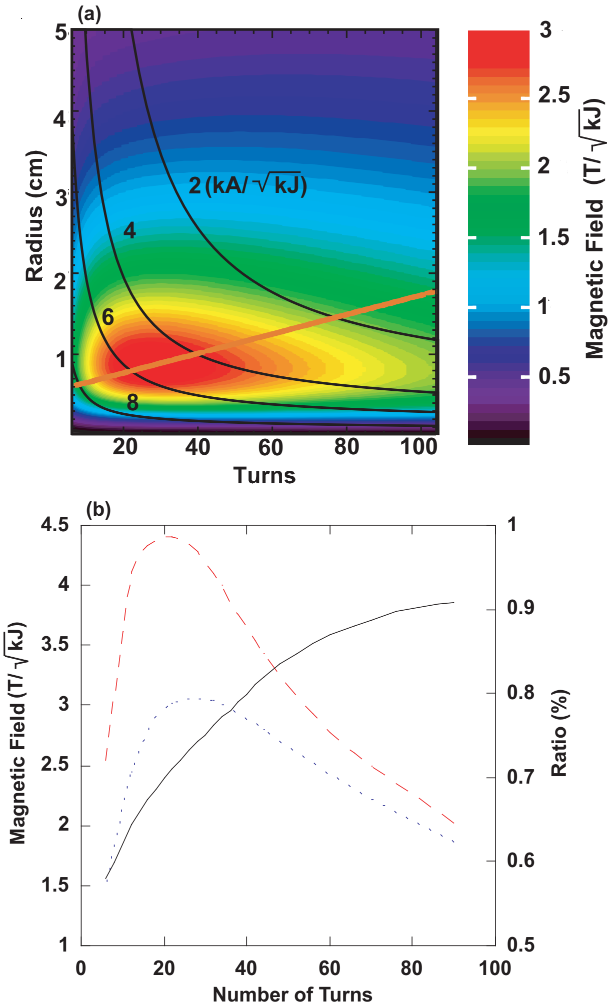

FIG. 4: (a) A contour plot of Equation 1 showing the normalized magnetic field strength as a function of the solenoid geometry. Also included are curves of constant current (black). The orange line passes through the maximum of Equation 1 and indicates the set of optimal designs when the material strength of the solenoid must be considered. (b) Ratio (solid) of the magnetic field produced between the coils (dotted) to the maximum field inside the solenoid (dashed) along the optimal line. The selection of a ratio defines the system geometry and the maximum field possible between the coils.